Pure appl. geophys. 163 (2006) 1751–1767
0033–4553/06/091751–17
DOI 10.1007/s00024-006-0095-1

Pure and Applied Geophysics

Experimental Evidence of Critical Sensitivity in Catastrophe

Xianghong Xu,[1] Mengfen Xia,[1,2] Fujiu Ke,[1,3] and Yilong Bai[1]

Abstract—The paper presents an experimental study on critical sensitivity in rocks. Critical sensitivity means that the response of a system to external controlling variable may become significantly sensitive as the system approaches its catastrophic rupture point. It is found that the sensitivities measured by responses on three scales (sample scale, locally macroscopic scales and mesoscopic scale) display increase prior to catastrophic transition point. These experimental results do support the concept that critical sensitivity might be a common precursory feature of catastrophe. Furthermore, our previous theoretical model is extended to explore the fluctuations in critical sensitivity in the rock tests.

Key words: Critical sensitivity, catastrophe, damage fraction, acoustic emission, digital speckle correlation method, fluctuation.

1. Introduction

Many observational evidences show that there are some precursors prior to a major earthquake, such as accelerating moment release (AMR) or power-law increase in the number of intermediate-size events (Jaumé *et al.*, 1999; Bowman *et al.*, 1998; Rundle *et al.*, 2000a), anomalously high values of Lurr (Yin *et al.*, 2000), etc.

Recently, based on statistical mesoscopic damage mechanics, Xia *et al.* (Xia *et al.*, 2002; Zhang *et al.*, 2004) suggested that the sensitivity of response to controlling variable might be an effective variable to characterize a system with macroscopic uncertainty. In particular, a properly defined sensitivity of the system may display significant increase as the system approaches its catastrophic point, i.e., the transition point from damage accumulation to catastrophic rupture. Such a behavior is called critical sensitivity. The underlying mechanism behind critical sensitivity is the

[1] State Key Laboratory of Nonlinear Mechanics (LNM), Institute of Mechanics, Chinese Academy of Sciences, Beijing 100080, PR China.
E-mail: xxh@lnm.imech.ac.cn; baiyl@lnm.imech.ac.cn
[2] Department of Physics, Peking University, Beijing 100871, PR China.
E-mail: xiam@lnm.imech.ac.cn
[3] Department of Applied Physics, BeiHang University, Beijing 100088, PR China.
E-mail: kefj@lnm.imech.ac.cn

coupling effect between disordered heterogeneity on multiple scales and dynamical nonlinearity due to damage-induced stress redistribution (STEIN, 1999; XIA *et al.*, 2000, 2002). Critical sensitivity may provide a clue to prediction of catastrophic transition, such as material failure or great earthquakes, provided the sensitivity of the system is measurable or can be monitored.

To validate the concept of critical sensitivity, a series of experiments have been conducted. 167 gabbro samples were tested under uniaxial compression. The deformation and damage processes were observed with acoustic emission (AE) and white Digital Speckle Correlation Method (DSCM) (PETER *et al.*, 1981; MA *et al.*, 2004) synchronously. Then, the sensitivities characterizing the evolution of damage, surface displacement pattern and AE energy induced by boundary displacement can be obtained. The experimental results show that these three kinds of responses of the samples become significantly sensitive to the controlling variable, i.e., boundary displacement, as the samples approach catastrophe. This clearly indicates that the experimental results do support the concept of critical sensitivity reasonably.

In addition, it can be seen that the sensitivities observed in the experiments display fluctuations, while the sensitivity obtained from the previous theoretical approximation (ZHANG *et al.*, 2004) is monotonic and smooth. In order to understand the mechanism governing the fluctuations in sensitivity, a model with multi-peak structure in the distribution function of mesoscopic units' threshold is introduced. It is found that the multi-peak structure might be responsible for the fluctuations shown in critical sensitivities.

2. Observations of Critical Sensitivity in Rock Failure

2.1 Experimental Method

In our tests, rectangular gabbro samples with dimensions of $5 \times 5 \times 13$ mm^3, were compressed uniaxially with a MTS810 testing machine. The loading mode is boundary-displacement control with velocity of 0.02 mm/min. The displacement was measured by an extensometer with resolution of 3 μm and an offset of 1 kN load.

The surface of the specimen was illuminated by a white luminescence and the speckle images were captured and transferred to a computer by a CCD camera. After the experiment, the speckle images were analyzed with DSCM, thus, both displacement and strain fields during the loading process were obtained.

Moreover, two AE sensors were fixed on two sides of a sample with a specially designed clamp. The resonant frequencies of the sensors are 140 kHz and 250 kHz, respectively. The AE signals were recorded and processed by an AE21C system produced by the Institute of Computer Technology of Shenyang, China. As well known, AE is an effective method to detect damage process of rock, so the AE series, such as AE energy, can provide statistical information on damage evolution.

2.2 Definitions of Critical Sensitivity Adopted in Rock Experiments

To deal with experimental data, a dimensionless boundary displacement U is adopted, i.e., $U = U^*/13$, where U^* is the actual boundary displacement. (Hereafter, symbols without superscript * will represent either dimensionless (like stress, displacement, length and energy, etc.) or normalized (like strain) variables, while those with * mean dimensional or non-normalized ones), and factor 13 is the length of the sample along the loading axis with unit of millimeter. Figure 1 shows the processed curves of actual nominal stress σ^{*P} versus dimensionless boundary displacement U^P for 151 gabbro samples (in the following text, symbols with superscript P demonstrate the processed experimental variables. See the processing method in Section 2.2.1). The catastrophe appears at the end of each curve. Clearly, it is hard to forecast when catastrophe will occur beforehand. In particular, the maximum and the failure stresses show large diversity. This macroscopic uncertainty results in great difficulty in rupture prediction.

In order to measure the sensitivity of a rock sample to external controlling variable, we define sensitivity S as

$$S = \frac{\Delta}{\Delta U}\left(\frac{\Delta R}{\Delta U}\right), \tag{1}$$

where the dimensionless boundary displacement U is the external controlling variable and R is the response of the rock sample. Moreover, in the theoretical model, if the second-order derivative of R, $\mathrm{d}^2R/\mathrm{d}U^2$, exists, Eq. (1) can be written as

$$S = \frac{\mathrm{d}^2R}{\mathrm{d}U^2}. \tag{1a}$$

In the present paper, R is defined as the accumulative response of the rock sample. Hence, the first-order derivative of R demonstrates the changing rate of the response

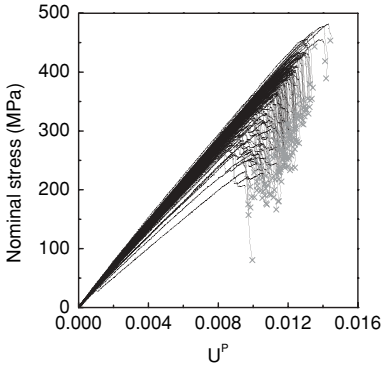

Figure 1
Processed curves of experimental nominal stress σ^{*P} versus dimensionless boundary displacement U^P for 151 gabbro samples under uniaxial compression. The symbols × indicate catastrophe points.

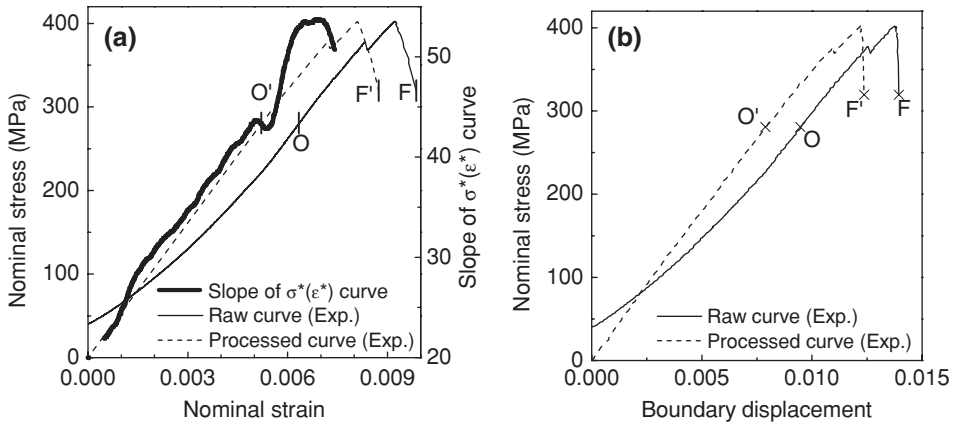

Figure 2
(a) The slope of $\sigma^*(\varepsilon^*)$ curve, namely $\Delta\sigma^*/\Delta\varepsilon^*$ (bulk solid line ▬). $\sigma^*(\varepsilon^*)$ (solid line –) and $\sigma^{*P}(\varepsilon^{*P})$ (dashed line – – –), are the raw and processed experimental nominal stress-strain curves respectively. (b) The curves, $\sigma^*(U)$ (solid line –) and $\sigma^{*P}(U^P)$ (dashed line – – –) are the raw and processed experimental nominal stress versus dimensionless boundary displacement curves, respectively. Points O and O′ are the points corresponding to maximum modulus, F and F′ are the catastrophe points.

with respect to the external controlling variable. In order to measure the sensitivity of the changing rate of the response to the external controlling variable, the second-order derivative of R is adopted as the definition of sensitivity, because it is considerably more sensitive to the external controlling variable than the first-order derivative.

Importantly, R could be chosen from different kinds of responses. In this paper, the responses from the behaviors at different scales is adopted, i.e., the mean damage fraction D at global scale, the distance ΔH^* between successive patterns of surface displacement related to the behavior at locally macroscopic scale and the AE energy Θ^* contributed from the events at mesoscopic scale. In data processing, D can be calculated from the experimental nominal stress σ^* and strain ε^* curve, ΔH^* can be calculated from the surface displacement patterns, and Θ^* can be obtained directly from the AE system, as discussed later in detail.

Critical sensitivity means that the response to the controlling variable, i.e., boundary displacement U, may become significantly sensitive, i.e., $S \gg 1$, prior to the catastrophe. Now, we focus on whether critical sensitivity is a common precursor to final rupture in rock experiments.

2.2.1 Sensitivity calculated from damage evolution

At the initial part of the raw experimental nominal stress σ^* and strain ε^* curve (Fig. 2(a), solid line), the slope of $\sigma^*(\varepsilon^*)$ curve, $\Delta\sigma^*/\Delta\varepsilon^*$ (Fig. 2(a), bulk solid line), increases with increasing ε^* due to the closure of micro-cracks. For simplicity, without regard to healing process of micro-cracks, only the weakness induced by

damage is considered based on damage mechanics (JAYATILAKA, 1979). Then, the global damage fraction D can be calculated from the processed σ^{*P} (ε^{*P}) curve obtained by the following steps (XU *et al.*, 2004): (1) Calculate the slope of $\sigma^*(\varepsilon^*)$ curve, $\Delta\sigma^*/\Delta\varepsilon^*$ (Fig. 2(a), bulk solid line), and suppose E_0^*, which equals to the maximum value of $\Delta\sigma^*/\Delta\varepsilon^*$ (at point O in Fig. 2(a)), as the initial elastic modulus of the rock sample. (2) Draw a straight line with slope E_0^* from the origin ($\sigma^{*P} = \varepsilon^{*P} = 0$) to O′ (O′ and O locate at the same nominal stress). (3) Parallelly shift the O-F-part of the raw stress-strain curve $\sigma^*(\varepsilon^*)$ to point O′. Then, the entire processed experimental nominal stress-strain curve $\sigma^{*P}(\varepsilon^{*P})$ (dashed line in Fig. 2(a)) is obtained. Similarly, parallelly draw the processed curve of nominal stress σ^{*P} versus boundary displacement U (solid line in Fig. 2(b)) from the origin ($\sigma^{*P} = U^P = 0$). Then, the processed experimental nominal stress σ^{*P} versus dimensionless boundary displacement U^P curve (dashed line in Fig. 2(b)) can be obtained.

Theoretically, global damage fraction D, a macroscopic variable characterizing damage evolution, can be obtained from the processed experimental nominal stress σ^{*P} and strain ε^{*P} curve based on mean field (MF) approximation. According to damage mechanics and MF approximation, the constitutive relation can be

$$\sigma^{*P} = \varepsilon^{*P} E_0^* (1 - D). \tag{2}$$

Then, global damage fraction D can be calculated by

$$D = 1 - \frac{\sigma^{*P}}{\varepsilon^{*P} E_0^*}. \tag{3}$$

The global damage fraction D of rock sample calculated from $\sigma^{*P}(\varepsilon^{*P})$ curve is shown in Figure 3(a). When choosing the response of R to be damage D, the sensitivity is denoted by S_D. Figure 3(b) shows the curve of S_D versus the boundary displacement U for a sample.

In order to compare the sensitivity series of different samples, a normalized boundary displacement U_0 is adopted,

$$U_0 = U/U_c, \tag{4}$$

where U_c is the dimensionless boundary displacement of a sample at its catastrophic point. Figure 3(c) shows the curves of S_D versus U_0 for 151 samples.

2.2.2 Sensitivity calculated from the distance between successive patterns of surface displacement

Since the length-pixel ratio of the imaging system is about 0.028 mm/pixel in DSCM system, the obtained displacement can be understood as an average over the area of 28×28 μm^2. The surface strain pattern can be calculated from the surface displacement pattern. Owing to damage evolution, the surface strain pattern becomes inhomogeneous on multi-scales, and later strain localization appears. Then, new

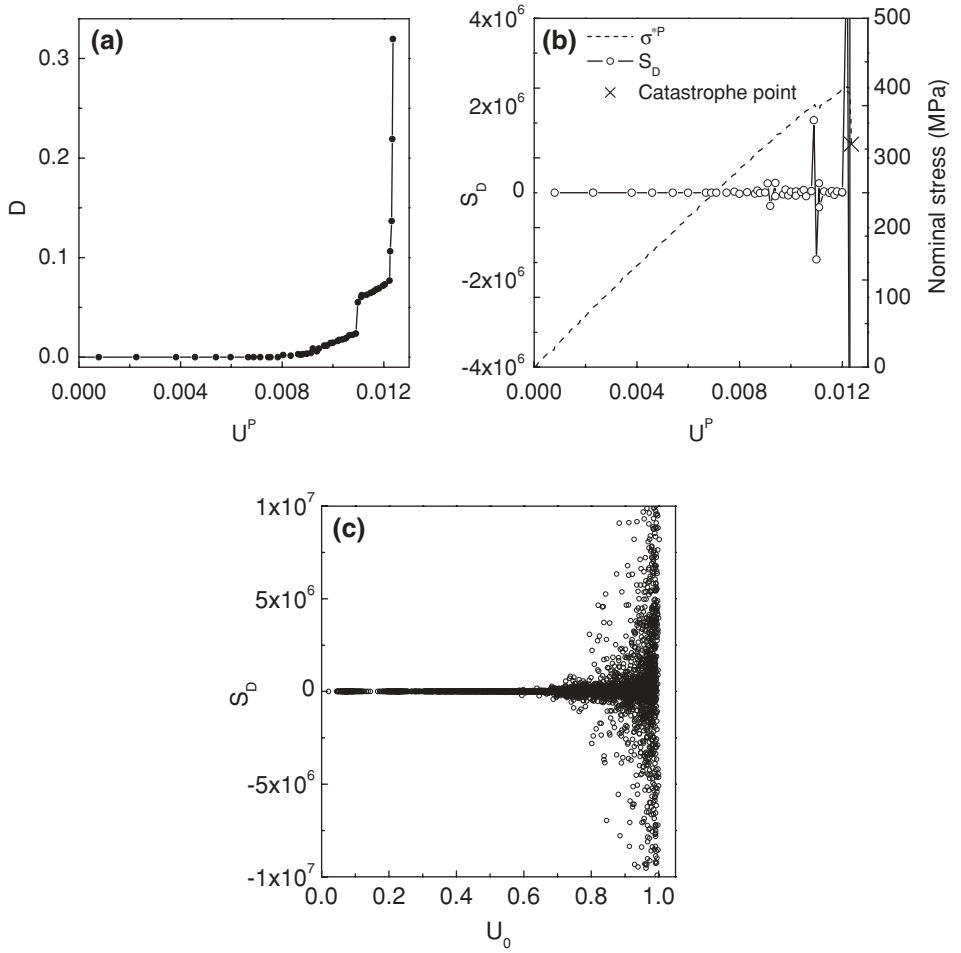

Figure 3

(a) Damage fraction D, obtained from experimental nominal stress-strain curves, versus processed boundary displacement U^{P}. (b) Sensitivity S_D calculated from damage evolution versus U^{P} for a sample. (c) S_D versus normalized boundary displacement U_0 for 151 samples.

scales between the pixel scale and the sample scale emerge. These emerging scales are called locally macroscopic scales in this paper. In order to describe the change of response of the system at the locally macroscopic scales, distance between the successive patterns of surface displacement is introduced. The distance between two patterns of surface displacement is defined as

$$\Delta H_i^* = \frac{1}{N_{\mathrm{eff}}} \sum_{x=1}^{131} \sum_{y=1}^{401} \left| \Delta u_i^*(x,y) \right|, \quad i = 1,2, \tag{5}$$

where $\Delta u_i^*(x,y)$ is the increment of surface displacement vector u_i^* at point (x,y) along axis i ($i = 2$ indicates loading direction whereas 1 the direction vertical to

loading), 131 and 401 are the number of points in the surface displacement pattern along axis 1 and axis 2, respectively, and N_{eff} is the number of points effective for DSCM calculation.

The curve of ΔH_1^* versus U^P is shown in Figure 4(a), and the sensitivity $S_{H_1^*}$ calculated from the distance between surface displacement patterns is shown in Figure 4(b) for a single sample and Figure 4(c) for 143 samples.

2.2.3 Sensitivity calculated from AE energy

Acoustic emission, resulted from mesoscopic damage evolution, is a response of rock sample to boundary displacement on the mesoscopic scale. AE energy is a

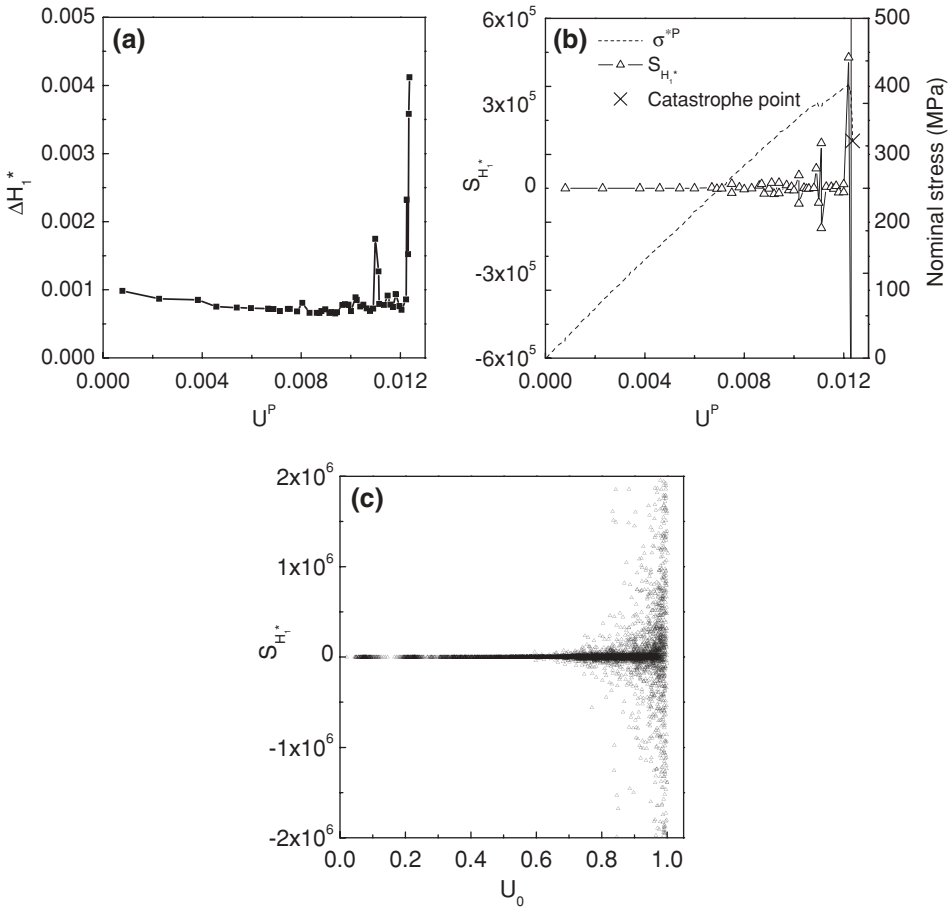

Figure 4
(a) The distance between surface displacement patterns ΔH_1^* versus U^P. (b) Sensitivity $S_{H_1^*}$ calculated from distance between surface displacement patterns versus U^P for a sample. (c) $S_{H_1^*}$ versus U_0 for 143 samples.

proper parameter characterizing damage and the accumulated AE energy Θ* can be obtained directly from AE recording, see Figure 5(a).

Then, taking response $R = \Theta^*$, the sensitivity S_{Θ^*} calculated from AE energy is shown in Figure 5(b) for a single sample and Figure 5(c) for 131 samples.

2.3 Critical Sensitivity in Rock Experiments

According to the above-mentioned method, the experimental results of sensitivity reflecting the responses on three scales are obtained, namely S_D, $S_{H_1^*}$ and S_{Θ^*} from the responses on sample scale, locally macroscopic scales and mesoscopic scale, respectively.

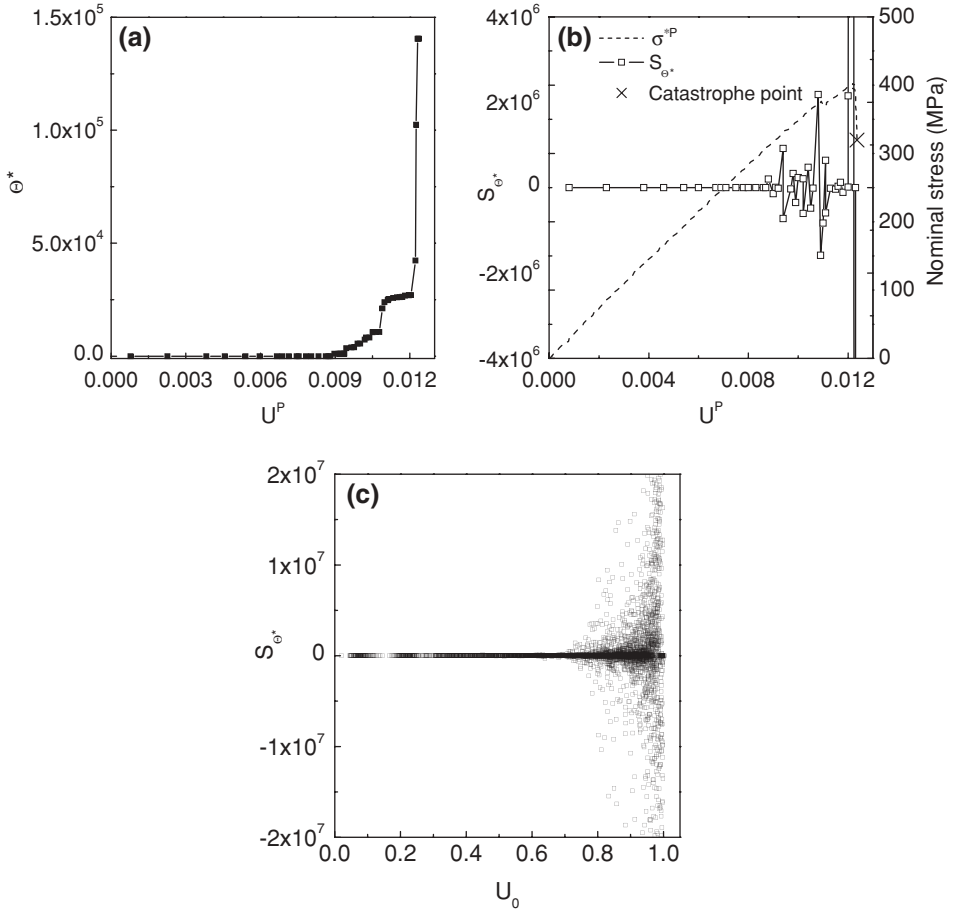

Figure 5
(a) Accumulative AE energy Θ* versus U^P. (b) Sensitivity S_{Θ^*} calculated from AE energy versus U^P for a sample. (c) S_{Θ^*} versus U_0 for 131 samples.

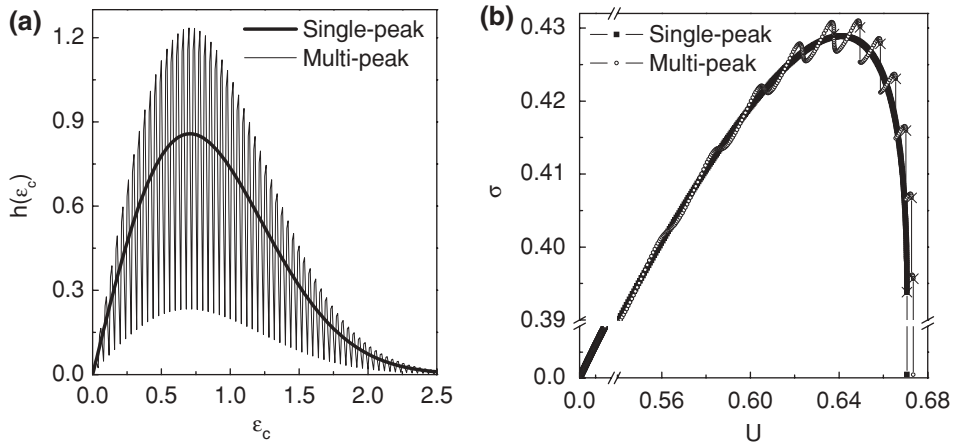

Figure 6
(a) Distribution function of mesoscopic strength ε_c, single-peak function with $m = 2$ in Eq. (29) (bulk solid line —) and multi-peak function with $m = 2$, $N = 100$, and $\Delta = 0.04$ in Eqs. (33)–(37) (solid line –). (b) Nominal stress σ versus boundary displacement U with $k = 0.3$ in Eq. (14), single-peak function (■ and corresponding line) and multi-peak function (○ and corresponding line).

Figures 3(b), 4(b), and 5(b) show the sensitivity S at the three scales for a single sample. At the initial stage, S_{Θ^*} is equal to zero since the events of mesoscopic damage are too small to be detected by AE sensors, $S_{H_1^*}$ and S_D are also equal to zero since the change of the surface displacement patterns is nearly zero and macroscopic damage can be neglected at the initial stage. In other words, at the initial stage, the responses of the system at all scales are not sensitive to the external controlling variable, i.e., the boundary displacement U. As the boundary displacement increases, the three sensitivities remain in low level. This means that the system is in a state with low sensitivity. However, the three sensitivities increase significantly prior to the catastrophic transition point. This implies that the system becomes highly sensitive prior to catastrophic point, from mesoscopic scale to macroscopic scale.

Figures 3(c), 4(c), and 5(c) show the three sensitivities for more than 100 samples. Noticeably, the series of sensitivities are different from sample to sample. That is to say, the catastrophic rupture demonstrates sample specificity. But, more importantly, there is a common trend in sensitivity for all samples, namely significantly increasing sensitivity near the catastrophic transition $U_0 = 1$. This is a strong experimental evidence of critical sensitivity prior to catastrophic rupture in heterogeneous rock.

Since the value of sensitivity of different samples displays large diversity, only a qualitative analysis can be given in present paper. In our later research, more quantitative work will be done.

3. Theoretical Analysis of Critical Sensitivity

However, it is noticeable that the sensitivity shows severe fluctuations in experiments (Figs. 3–5). In order to explore the mechanism underlying the fluctuations of sensitivity in rock experiments, a theoretical model is proposed to explain the phenomenon. Suppose the rock sample and the MTS tester, be two parts in series and driven by boundary displacement quasi-statically. According to MF approximation, the boundary displacement equals to

$$U^* = L^*\varepsilon^* + L_e^*\varepsilon_e^*, \tag{6}$$

where ε^* and ε_e^* are nominal strains of the rock sample and the elastic tester respectively, while L^* and L_e^* are the corresponding initial length along the loading axis of the two parts. Under uniaxial monotonic loading, the equilibrium condition between the rock sample and the elastic part can be written as

$$\sigma^* = \varepsilon_e^* E_e^* = \varepsilon^* E_0^*(1 - D), \tag{7}$$

where σ^* is the nominal stress, E_e^* is the elastic modulus of the tester, and E_0^* is the initial elastic modulus and D is the damage of the rock sample. According to damage mechanics, the true stress σ_s^* and true strain ε_s^* of the rock sample are respectively given by

$$\sigma_s^* = \frac{\sigma^*}{1 - D} \quad \text{and} \quad \varepsilon_s^* = \varepsilon^*. \tag{8}$$

After taking dimensionless stress σ and normalized strain ε,

$$\sigma = \sigma^*/\eta^*, \quad \varepsilon = E_0^*\varepsilon^*/\eta^* \ \text{ and } \ \varepsilon_e = E_e^*\varepsilon_e^*/\eta^*, \tag{9}$$

where η^* is the position factor of Weibull distribution (WEIBULL, 1951) (see Eq. (28)). According to Eqs. (7)–(9), the relations between the nominal and true variables, i.e., stress, strain and damage of the damage part, are

$$\sigma = \varepsilon(1 - D), \tag{10}$$

$$\sigma = \sigma_s(1 - D) \quad \text{and} \quad \varepsilon = \varepsilon_s, \tag{11}$$

$$\sigma_s = \varepsilon_s. \tag{12}$$

According to Eqs. (7) and (9), the relations between dimensionless nominal stress and normalized strain ε_e of the elastic part can be

$$\sigma = \varepsilon_e. \tag{13}$$

According to Eqs. (6) and (9), the dimensionless boundary displacement U can be derived as

$$U = \frac{U^*}{\eta^*\left(\frac{1}{E_0^*/L^*} + \frac{1}{E_e^*/L_e^*}\right)} = \frac{1}{k+1}(k\varepsilon + \sigma) = \frac{k+1-D}{k+1}\varepsilon, \tag{14}$$

where k is the ratio between the rigidity of the elastic part and the initial rigidity of the rock sample

$$k = \frac{E_e^*/L_e^*}{E_0^*/L^*}. \tag{15}$$

As soon as damage occurs in heterogeneous elastic-brittle medium, some stored energy will be released. Since the elastic energy of the elastic-brittle (without residual deformation) model under MF approximation

$$\Theta_{el}(\varepsilon) = \frac{1}{2}\sigma\varepsilon = \frac{1}{2}(1-D)\varepsilon^2, \tag{16}$$

and the increment of external work on rock sample is

$$\Delta W = \sigma\Delta\varepsilon = (1-D)\varepsilon\Delta\varepsilon. \tag{17}$$

Then, the increment of energy release can be

$$\Delta\Theta(\varepsilon) = \Delta W(\varepsilon) - \Delta\Theta_{el}(\varepsilon) = \frac{\varepsilon^2}{2}\Delta D. \tag{18}$$

Suppose the rock sample can be simplified as a driven, nonlinear threshold system (RUNDLE *et al.*, 2000b; ZHANG *et al.*, 2004), comprising numerous interacting and nonlinear mesoscopic units, which fails when the force acting on it reaches a predefined threshold. In the present model, it is assumed that all units have the same elastic modulus E_0^* but different breaking stress threshold σ_c^*. Hence, firstly, each unit remains elastic until its own σ_c^*, i.e.,

$$\sigma_s^* = \varepsilon_s^* E_0^*, \tag{19}$$

where σ_s^* and ε_s^* are mesoscopic stress and strain of each unit, i.e., true stress and true strain as mentioned before, respectively. According to Eq. (19), the stress threshold σ_c^* and strain threshold ε_c^* of the mesoscopic unit should also follow

$$\sigma_c^* = \varepsilon_c^* E_0^*. \tag{20}$$

According to definitions (9), the relations between the dimensionless stress threshold σ_c and normalized strain threshold ε_c can be

$$\sigma_c = \varepsilon_c. \tag{20a}$$

Secondly, as soon as σ_s^* reaches σ_c^* on a unit, the unit will be broken and can never support load, i.e.,

$$\sigma_s^* = \sigma_s = 0, \tag{21}$$

when the unit is broken.

Suppose that at the initial state the mesoscopic strength ε_c of units follows a certain type of distribution function $h(\varepsilon_c)$, which should be normalized as

$$\int_0^\infty h(\varepsilon_c)\mathrm{d}\varepsilon_c = 1. \tag{22}$$

For quasi-static loading, i.e., the characteristic time of damage relaxation is much shorter than that of loading, damage D in Eq. (7) can be determined by

$$D = \int_0^\varepsilon h(\varepsilon_c)\mathrm{d}\varepsilon_c. \tag{23}$$

According to Eqs. (1a), (10), (14), (17), and (23), the sensitivities of damage, nominal strain and released energy can be respectively derived as

$$S_D = \frac{\mathrm{d}^2 D}{\mathrm{d}U^2} = \frac{(k+1)^2\left[(k+1-D)h'(\varepsilon) + 2(h(\varepsilon))^2\right]}{(k+1-D-\varepsilon h(\varepsilon))^3}, \tag{24}$$

$$S_\varepsilon = \frac{\mathrm{d}^2\varepsilon}{\mathrm{d}U^2} = \frac{(k+1)^2[2h(\varepsilon) + \varepsilon h'(\varepsilon)]}{(k+1-D-\varepsilon h(\varepsilon))^3}, \tag{25}$$

and

$$S_\Theta = \frac{\mathrm{d}^2\Theta}{\mathrm{d}U^2} = \frac{(k+1)^2\varepsilon(\varepsilon h'(\varepsilon) + 2h(\varepsilon))(k+1-D)}{2(k+1-D-\varepsilon h(\varepsilon))^3}, \tag{26}$$

where

$$h'(\varepsilon) = \frac{\mathrm{d}h(\varepsilon)}{\mathrm{d}\varepsilon}. \tag{27}$$

Under the MF approximation, S_ε is equivalent to $S_{H_1^*}$ which was defined for the experiments before.

From Eqs. (24), (25), and (26), it can be seen that all sensitivities are dependent on the distribution function $h(\varepsilon_c)$. Next, the effect of distribution function, such as single-peak distribution function and multi-peak distribution function, on sensitivity will be discussed.

(a) Single-peak distribution function, for example, Weibull distribution function (WEIBULL, 1951)

$$h^*\left(\sigma_c^*\right) = \frac{m}{\eta^*}\left(\frac{\sigma_c^*}{\eta^*}\right)^{m-1} e^{-\left(\frac{\sigma_c^*}{\eta^*}\right)^m}, \tag{28}$$

or its normalized form

$$h(\sigma_c) = h(\varepsilon_c) = m\varepsilon_c^{m-1} e^{-\varepsilon_c^m}, \tag{29}$$

where m is the shape factor and η^* is the position factor of Weibull distribution. For Weibull distribution, the three sensitivities, S_D (Eq. (24)), S_ε (Eq. (25)), and S_Θ (Eq. (26)) can be expressed by

$$S_D = \frac{(k+1)^2 m\varepsilon^{m-2} e^{-\varepsilon^m}\left[(m-1-m\varepsilon^m)\left(k+e^{-\varepsilon^m}\right)+2m\varepsilon^m e^{-\varepsilon^m}\right]}{\left(k+(1-m\varepsilon^m)e^{-\varepsilon^m}\right)^3}, \tag{30}$$

$$S_\varepsilon = \frac{(k+1)^2 m\varepsilon^{m-1} e^{-\varepsilon^m}(m+1-m\varepsilon^m)}{\left(k+(1-m\varepsilon^m)e^{-\varepsilon^m}\right)^3}, \tag{31}$$

and

$$S_\Theta = \frac{(k+1)^2 m\varepsilon^m e^{-\varepsilon^m}(m+1-m\varepsilon^m)\left(k+e^{-\varepsilon^m}\right)}{2\left(k+(1-m\varepsilon^m)e^{-\varepsilon^m}\right)^3}. \tag{32}$$

(b) Multi-peak distribution function

$$\tilde{h}(\varepsilon_c) = \sum_{i=1}^{N} a_i \frac{m_i}{\eta_i}\left(\frac{\varepsilon_c - b_i}{\eta_i}\right)^{m_i-1} e^{-\left(\frac{\varepsilon_c-b_i}{\eta_i}\right)^{m_i}} \theta(\varepsilon_c - b_i), \tag{33}$$

where N, m_i, a_i, b_i, and η_i ($i = 1, 2, \ldots, N$) are undetermined coefficients and

$$\theta(x) = \begin{cases} 1 & x \geq 0 \\ 0 & x < 0 \end{cases}. \tag{34}$$

Suppose $m_i = m$, and b_i, a_i, and η_i be determined as follows. Give a definite interval $\Delta > 0$ and let

$$b_i = (i-1)\Delta, \quad i = 1, 2, \ldots N \text{ and } b_{N+1} = \infty. \tag{35}$$

In accordance with Eqs. (29) and (33),

$$a_i = \int_{b_i}^{b_{i+1}} h(\varepsilon_c)\mathrm{d}\varepsilon_c = e^{-b_i^m} - e^{-b_{i+1}^m}, \tag{36}$$

and

$$\eta_i = \left(\int_{b_i}^{b_{i+1}} \varepsilon_c h(\varepsilon_c)\mathrm{d}\varepsilon_c \Big/ a_i - b_i\right) \Big/ \Gamma\left(1+\frac{1}{m}\right). \tag{37}$$

In this situation, it can be easily seen that the two distribution functions satisfy the unitary condition Eq. (22) and have the same mean value

$$\int_0^\infty \varepsilon_c h(\varepsilon_c)\mathrm{d}\varepsilon_c = \int_0^\infty \varepsilon_c \tilde{h}(\varepsilon_c)\mathrm{d}\varepsilon_c. \tag{38}$$

Clearly, there is $\tilde{h}(\varepsilon_c) = h(\varepsilon_c)$ as $N = 1$ and $\Delta \to \infty$, i.e. $h(\varepsilon_c)$ is a special sample of $\tilde{h}(\varepsilon_c)$. Figure 6(a) shows the distribution function of mesoscopic strength, single-peak distribution function $h(\varepsilon_c)$ with $m = 2$ (bulk solid line) and multi-peak distribution function $\tilde{h}(\varepsilon_c)$ with $m = 2$, $N = 100$, and $\Delta = 0.04$ (solid line). Figure 6(b) shows the curves of normalized nominal stress σ versus dimensionless boundary displacement U with $k = 0.3$, single-peak distribution function (■ and corresponding line) and multi-peak distribution function (○ and corresponding line). Clearly, many small events appear prior to final catastrophe with multi-peak distribution function, while there is only final catastrophe with single-peak distribution function. Thus, the damage fraction D, nominal strain ε and the released energy Θ are continuous and smooth functions of boundary displacement prior to final catastrophe (■ and corresponding line in Figures 7(a), 8(a), and 9(a)) for the case of single-peak distribution function, but discontinuous for multi-peak distribution function (○ and corresponding line in Figs. 7(a), 8(a), and 9(a)).

The variations of sensitivities, S_D, S_ε, and S_Θ, versus dimensionless boundary displacement U are shown in Figures. 7(b), 8(b), and 9(b). It is found that S_D, S_ε, and S_Θ for the two different distribution functions display critical sensitivity, that is to say, they increase sharply prior to catastrophic rupture. It can also be seen that, in the case of single-peak distribution function $h(\varepsilon_c)$, the sensitivity is monotonic and smooth (■ and corresponding line in Figs. 7(b), 8(b), and 9(b)), but the sensitivity for multi-peak distribution function displays fluctuations (○ and corresponding line in Figs. 7(b), 8(b), and 9(b)). Since the distribution function of real materials may present complicated structure and cannot be modeled by a continuous single-peak function, the distribution function with multiple peaks might be more appropriate to

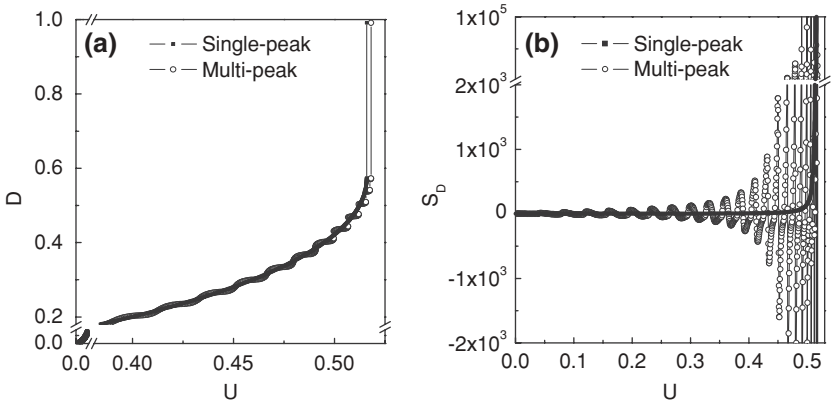

Figure 7
(a) Damage fraction D versus boundary displacement U. (b) Sensitivity S_D calculated from damage. In (a) and (b), single-peak function (■ and corresponding line) and multi-peak function (○ and corresponding line).

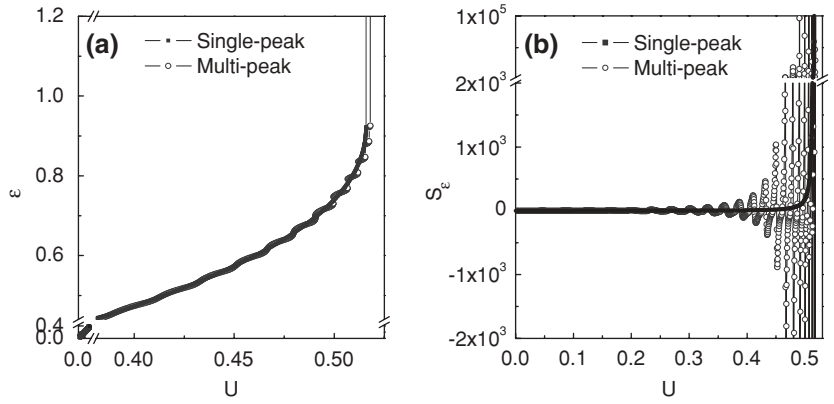

Figure 8
(a) Nominal strain ε versus U. (b) Sensitivity S_ε calculated from nominal strain. In (a) and (b), single-peak function (■ and corresponding line) and multi-peak function (○ and corresponding line).

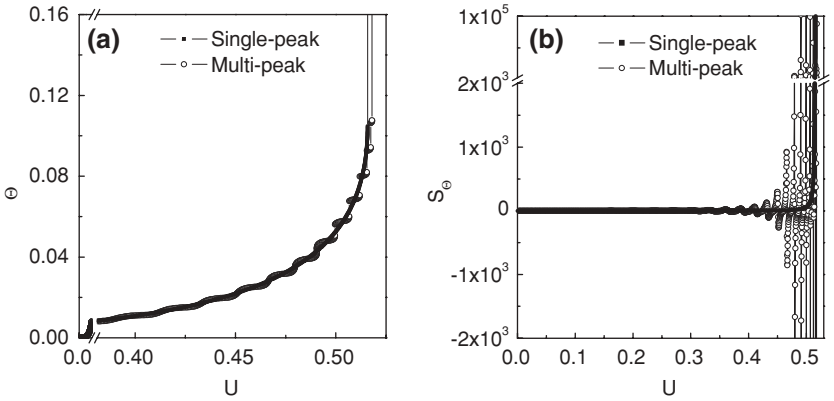

Figure 9
(a) Accumulated released energy Θ versus U. (b) Sensitivity S_Θ calculated from released energy. In (a) and (b), single-peak function (■ and corresponding line) and multi-peak function (○ and corresponding line).

represent real materials, and the corresponding results are more similar to that observed in experiments. Thus, the multi-peak structure of the distribution function might be the reason for the fluctuations shown in the critical sensitivity.

4. Conclusions

The prediction of catastrophic rupture, like forecasting of large earthquakes or prediction of materials failure, is a problem of great scientific and societal concern.

However, it is also a very difficult problem due to its richness of dynamical complexity. A possible approach to catastrophe prediction is to search universal features of catastrophe. Based on analytical and numerical studies, it is found that critical sensitivity might be a common precursory feature of catastrophe in heterogeneous brittle media, and to monitor the sensitivity of a system may give helpful clues to rupture prediction.

Experimental studies on critical sensitivity are presented in this paper. It is found that: (1) critical sensitivity is a common precursor prior to catastrophic rupture; (2) the observed fluctuations in sensitivity can be attributed to the multi-peak structure of the distribution function of mesoscopic strain threshold. These results provide experimental evidence for critical sensitivity.

The series of sensitivity presents sample specificity, i.e., they are different from sample to sample for similar samples under the same loading condition. In particular, the maximum values of sensitivity prior to catastrophe show strong diversity for these samples. It is inappropriate to predict catastrophe based on a common threshold of the sensitivity. We think that an effective method of catastrophe prediction might be based on the universal behaviors of sensitivity as the system is approaching its catastrophic transition point. For example, a theoretical analysis shows that, in the case of fast loading, the sensitivity displays a peak prior to catastrophic rupture (ZHANG *et al.*, 2004). The catastrophe prediction in the case of fast loading might be based on the appearance of the peak in the sensitivity curve. The experimental study of loading effect on critical sensitivity will be discussed in another paper.

Acknowledgements

This work is supported by the National Natural Science Foundation of China (Grant No. 10172084, 10232050, 10372012 and 10472118) and the Major State Research Project "Nonlinear Science" G200007735. The authors would like to thank Haisheng Yang for assistance with the experimentation and Dr Can Yin for editing this paper for grammar.

REFERENCES

BOWMAN, D.D., OUILLON, G., SAMMIS, C.G., SORNETTE, A., and SORNETTE, D. (1998), *An observation test of the critical earthquake concept*, J. Geophys. Res. *103*, 359–372.

JAYATILAKA, A.S., *Fracture of Engineering Brittle Materials*. (Applied Sciences Publishers Ltd., London, 1979).

JAUMÉ, S.C. and SYKES L.R. (1999), *Evolving towards a critical point: A review of accelerating seismic moment/energy release prior to large and great earthquakes*, Pure Appl. Geophys. *155*, 279–305.

MA, S.P., XU, X.H., and ZHAO, Y.H. (2004), *The Geo-DSCM system and its application to the deformation measurement of rock materials*, Int. J. Rock Mech. Mining Sci. *41*, 411–412.

PETER, W.H. and RANDSON, W.F. (1981), *Digital imaging techniques in Experimental stress analysis*, Opt. Eng. *21*, 427–431.

RUNDLE, J.B. (2000a), *Precursory seismic activation and critical-point phenomena*, Pure Appl. Geophys. *157*, 2165–2182.

RUNDLE, J.B. and KLEIN, W. (2000b), *Linear pattern dynamics in nonlinear threshold systems*, Phys. Rev. E *61*, 2418–2431.

STEIN, R.S. (1999), *The role of stress transfer in earthquake occurrence*, Nature *402*, 605–609.

WEIBULL, W. (1951), *A statistical distribution function of wide applicability*, J. Appl. Mech. ASME *18*, 293–297.

XIA, M.F., KE, F.J., and BAI, Y.L. (2000), *Evolution induced catastrophe in a nonlinear dynamical model of materials failure*, Nonlinear Dynamics *22*, 205–224.

XIA, M.F., WEI, Y.J., KE F.J., and BAI, Y.L. (2002), *Critical sensitivity and transscale fluctuations in catastrophe rupture*, Pure Appl. Geophys. *159*, 2491–2509.

XU, X.H., MA, S.P., XIA, M.F., KE, F.J., and BAI, Y.L. (2004), *Damage evaluation and damage localization of rock*, Theor. Appl. Fract. Mech. *42*, 131–138.

YIN, X.C., WANG, Y.C., PENG, K.Y., BAI, Y.L., WANG, H.T., and YIN, X.F. (2000), *Development of a new approach to earthquake prediction: Load/Unload Response Ratio (LURR) Theory*, Pure Appl. Geophys. *157*, 2365–2383.

ZHANG, X.H., XU, X.H., XIA, M.F., and BAI, Y.L. (2004), *Critical sensitivity in driven nonlinear threshold systems*, Pure Appl. Geophys. *161*, 1931–1944.

(Received November 12, 2004, revised October 6, 2005, accepted November 7, 2005)